Anomalous Optical Propagation and Potential Sensitivity Enhancement in a Micro-Coil Resonator Based on Microfiber

Feilin Zhang and Xiyuan Chen

***Abstract*—The resonance characteristics of the micro-coil resonator(MCR) with different turns and coupling conditions are presented, which show that the effective length of the MCR with small coupling coefficient at primary resonant is independent of the turns, and the resonance dips always appear in pairs corresponding to multiple critical-coupling because of the periodicity of coupling strength. However, complicated resonance is observed in an MCR with larger coupling coefficient and turns. The superluminal or subluminal propagation regime can be obtained respectively by adjusting the coupling condition, and the effect of loss on them in different coupling conditions is investigated. There is such a loss threshold in the critical-coupling and over-coupling conditions, near which the group refractive index abrupt changes between positive and negative extremum, and the threshold is increased by 10^5 orders of magnitude under over-coupling condition compared with critical-coupling. In view of the transmission near a resonant evolve not only with the detuning of transmission phase, but also drastically with the adjustment of coupling condition which will be modulated by the cladding refractive index and coupling length. Hence a potential sensitivity enhancement for biochemical and inertial sensing based on MCR is also investigated briefly.**

***Index Terms*—Micro-coil resonator, superluminal and subluminal propagation, coupling condition, sensitivity enhancement.**

I. Introduction

MICROFIBER with a diameter of micron order, which is fabricated from standard optical fiber usually by fused biconical taper technique, are particularly suited for fabricating optical resonance device due to their flexibility, large evanescent fields and ease of bending without any measurable losses [1]. Various types of resonators based on microfiber have been proposed, such as micro loop resonator [2], [3], micro knot resonator [4] and micro-coil resonator(MCR) [5]. Different from other types, MCR is an alternative three-dimensional resonator, as shown in Fig. 1, which can be wound on a dielectric rod with relatively low refractive index for support. In such a configuration, the optical beam propagates along the axis of the micro-fiber, while coupling between adjacent micro-fibers. That is to say, inter-turn coupling occurs on the whole MCR, which makes the coupling region of MCR much larger than that of other planar single-ring resonators, and the response of light–matter interaction maybe also different. Thanks to the loss of microfiber is expected to be as small as that of microcavity based on precision manufacturing, the MCR made of microfiber could have a quality factor comparable to that of the whispering gallery mode microcavity potentially, i.e.,$Q\sim10^{10}$ [5], [6]. Moreover, the MCR can be composed of a single uniform fiber so that its internal transmission loss is much lower due to no splicing, and it has good compatibility with other optical devices, such as laser, phase modulator, photodetector, etc. At present, high quality factor MCR has been demonstrated by many scholars [7], and the Q factor can be improved by increasing the number of turns or layers [8], [9]. Much attention has been drawn to the study of MCR due to such high-quality factor makes it potential applications in numerous fields, such as nonlinear optics, optical sensing, optical amplifier and quantum computing [10]–[12].

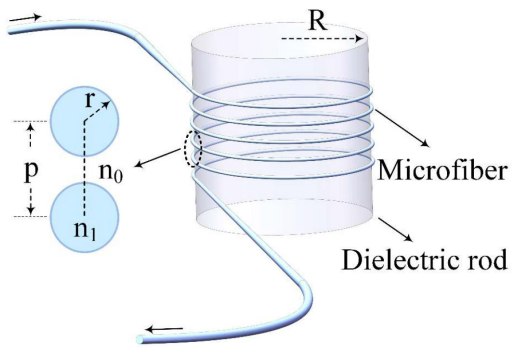

Fig. 1. Schematic and the local cross section of a uniform MCR. R and r are the radii of MCR and micro fiber respectively, n_0 and n_1 are the refractive indices of the substrate and the micro fiber respectively, p is the pitch between adjacent microfibers.

Controlling and modifying the velocity of light induced by the dispersion in resonator also has always been a subject of intense research due to the attractive application prospects in optical buffer, tunable optical delay lines, optical memories, all-optical switches and quantum information processing [13]–[17]. Naturally, MCR has attracted the attention of many scholars as a device to control of the structured light [18]. The dispersion characteristic of the MCR with inter-turn coupling configuration is complicated and distinctive due to the existence of both

Manuscript received May 31, 2021; revised June 17, 2021; accepted June 17, 2021. Date of publication June 22, 2021; date of current version July 12, 2021. *(Corresponding author: Xiyuan Chen.)*

The authors are with the Key Laboratory of Micro-Inertial Instrument and Advanced Navigation Technology Ministry of Education, School of Instrument Science and Engineering, Southeast University, Nanjing, Jiangsu 210096, China (e-mail: zhangfeilin@seu.edu.cn; chxiyuan@seu.edu.cn).

Digital Object Identifier 10.1109/JPHOT.2021.3091146

structural dispersion and coupling dispersion, especially for the MCR with multiple turns [19], [20]. However, the dispersion study of MCR is mostly focused on normal dispersion and subluminal propagation, the abnormal dispersion and superluminal propagation in MCR are rarely mentioned [19], [21], [22].

On the other hand, various sensor applications based on MCR have been explored experimentally and theoretically, such as refractometric sensing [23]–[25], current sensing [26], magnetic field sensing [27], angular velocity sensing [28]. Notice that the sensitivity response is different for different sensing mechanism when operating the resonator under superluminal or subluminal propagation regime. The recently accepted conclusion is the subluminal propagation regime corresponds to the longer transit time, which is beneficial to the sensing based on light–matter interaction, such as biochemical sensing. While the subluminal propagation regime corresponds to the anomalous structure dispersion, which is beneficial to the inertial sensing, such as optical gyroscope. Furthermore, the coupling condition of the MCR is sensitive to coupling coefficient and coupling length due to the strong evanescent field effect and large coupling region, and the resonance characteristic is closely related to the coupling condition. That is to say, the resonance state is modified not only by the detuning of the transmission phase like planar single-ring resonator, but also by the change of the coupling coefficient and coupling length, which suggests its potential sensitivity enhancement in sensing applications.

In this paper, we aim to study the anomalous optical propagation and potential sensitivity enhancement of MCR with different coupling conditions and turns. In what follows, the theoretical model of a uniform MCR with N turns is described firstly, and the transmission of the lossy MCR with different turns are presented. After simulation of the dispersion characteristics under different coupling conditions, such as group delay, group velocity and group refractive index, the dependences of superluminal and subluminal propagation regime on the coupling and loss coefficient are analyzed. In view of the special transmission characteristics and the mechanism of biochemical and inertial sensing based on the MCR, a potential sensitivity enhancement for biochemical and inertial sensing based on MCR is also investigated briefly.

II. The Theoretical Model and Transmission Characteristics of MCR

The schematic and the local cross section of a uniform MCR is shown in Fig. 1, where a biconical microfiber with radius r is wound around a dielectric rod by micromanipulation. Practically, the dielectric rod can be removed after wrapping, and then the MCR is packaged with lower refractive index material as substrate [29]. The light propagation in the coupled system can be analyzed by perturbation method. The microfiber diameter is comparable to the radiation wavelength, so self-coupling will be generated between co-propagating light in the adjacent turns of the micro-coil with appropriate pitch. Moreover, MCR diameter is much larger than the microfiber diameter, and the adiabatic approximation of parallel transport can be applied in MCR because of the characteristic transversal dimension of propagating mode in the microfiber is much smaller than the characteristic bend radius in practice. Therefore, the light propagation round a uniform MCR with N turns is described by the following coupled-wave equations based on Sumetsky's analysis [5]:

$$\frac{d}{ds}\begin{pmatrix} A_1(s) \\ A_2(s) \\ \vdots \\ A_{N'}(s) \\ \vdots \\ A_{N-1}(s) \\ A_N(s) \end{pmatrix} = \begin{pmatrix} 0 & ik & 0 & \cdots & 0 & 0 & 0 \\ ik & 0 & ik & \cdots & 0 & 0 & 0 \\ 0 & ik & 0 & \cdots & 0 & 0 & 0 \\ \vdots & \vdots & \vdots & \vdots & \vdots & \vdots & \vdots \\ 0 & 0 & 0 & \cdots & 0 & ik & 0 \\ 0 & 0 & 0 & \cdots & ik & 0 & ik \\ 0 & 0 & 0 & \cdots & 0 & ik & 0 \end{pmatrix} \begin{pmatrix} A_1(s) \\ A_2(s) \\ \vdots \\ A_{N'}(s) \\ \vdots \\ A_{N-1}(s) \\ A_N(s) \end{pmatrix} \tag{1}$$

where $A_N(s)$ is the slowly varying amplitude of the electric field in the *Nth* coil at a distance *s* round the coil, and k is the coupling coefficient between two adjacent microfibers. Note that the output of the previous turn is the input of the next turn since the MCR is a continuous spiral structure as depicted in Fig. 1. Therefore, the boundary conditions can be expressed as:

$$A_{N'+1}(0) = A_{N'}(L)\exp(i\beta L),\ N' = 1, 2, \ldots N-1 \tag{2}$$

where β is the propagation constant of fundamental mode along the microfiber and L is the length of each coil. The input electric field amplitude to the coil is given by $A_1(0)$, while the output electric field amplitude is given by $A_N(L)$. Then, the amplitude transmission coefficient can be expressed as:

$$T = \frac{A_N(L)}{A_1(0)} e^{i\beta L} \tag{3}$$

it can be solved by using the matrix method according to reference [20]. Furtherly, the light power transmittance of the system can be expressed as:

$$P = |T|^2 \tag{4}$$

Then, the phase of the transmission amplitude can be obtained by:

$$\varphi_T = \arg(T) = \mathrm{Im}[\ln(T)] \tag{5}$$

and the group delay can be expressed as:

$$t_d = \frac{d\varphi_T}{d\omega} = \frac{L_{eff}}{c}\frac{d\varphi_T}{d\varphi} \tag{6}$$

where *c* is the velocity of light in vacuum, φ is the one round-trip phase shift, $L_{eff} = c \cdot \tau_0$is the effective length of the MCR, which is defined as the product of c and the transit time τ_0. Thus, the group velocity can be defined as the effective length of the MCR divided by the group delay: $V_g = L_{eff}/t_d$. Obviously, the group velocity V_g is phase dependent, and the resonances will be observed when the following conditions are satisfied:

$$\varphi = \beta L_{eff} = 2m\pi + \frac{\pi}{2} \tag{7}$$

where m is an integer. If the MCR is assumed to be lossless, then $P = 1$, the light waves propagating in the MCR are all-pass and the resonance of MCR is reflected in the group delay only [30], [31]. Nevertheless, losses in the MCR arise from small bend

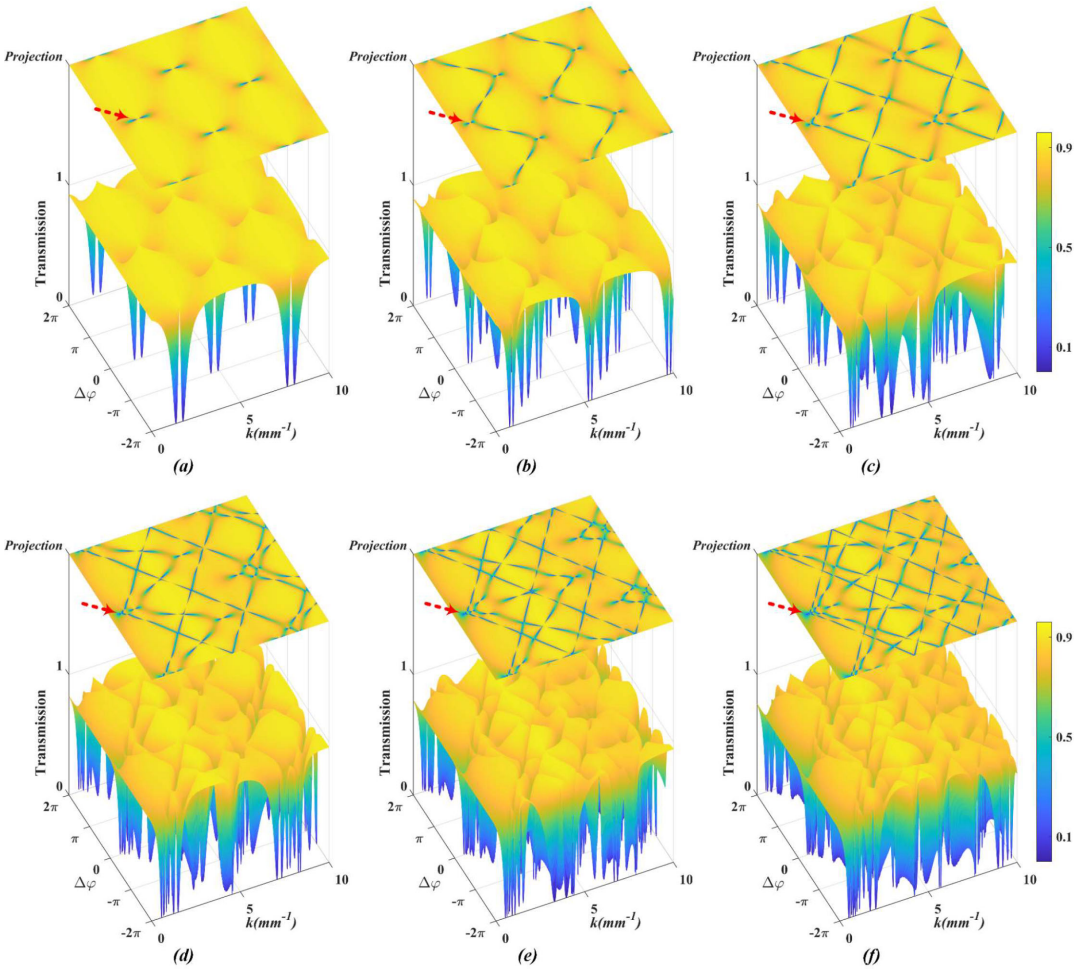

Fig. 2. The dependence of the transmission of the MCR with (*a*)∼(*f*): 2∼8 turns on the transmission phase and coupling coefficient when $L = 1mm$ and $\alpha = 0.02/mm$ are assumed. The primary resonance regimes are marked by red arrows.

radius, surface scattering and material absorption are unavoidable actually, and one can describe the effects of loss through an imaginary propagation constant $\beta = 2\pi n_{eff}/\lambda + i\alpha$, where n_{eff} is the effective refractive index, λ is the optical wavelength, α represents the optical loss coefficient.

The transmission characteristics of MCR has been studied by many scholars. As a reference, the transmission spectra of an MCR with different turns has been demonstrated in Fig. 3 of reference [32]. It depicts that the free spectral range(FSR) and resonance wavelength of MCR are independent of the number of turns when the MCR parameters are taken as:$k = 0.5/mm$, $L = 1mm$,$\alpha = 0.02/mm$, which means that the effective length L_{eff} of MCR is independent of the number of turns (i.e., $L_{eff} \neq N \cdot L$). However, the transmission spectra become different and complicated relatively with the coupling coefficient increasing as shown in Fig. 2, in which the dependence of the transmission characteristics of the MCR with different turns on the coupling coefficient and transmission phase are revealed by numerical simulation. $L = 1mm$ and $\alpha = 0.02/mm$ are still assumed in this paper for the convenience of comparison. The projection profiles (equivalent to the top views) of the transmission spectrum are depicted on the top of each sub-image separately, and $\Delta\varphi$ is the detuning of one round-trip phase of the incident beam to the fundamental resonant phase. Obviously, the projection profiles evolve more and more complicated as the coupling coefficient and the number of turns increasing. The resonance occurs generally when the transmission phase delay is an integral multiple of 2π for a conventional ring resonator, but not for an MCR with a large enough coupling coefficient. It suggests that the beam ascends and descends the MCR by coupling from one microfiber to the one near it, rather than traveling round and round along the coil. Multi-beam interference will be caused in the propagation of light between different turns when the coupling strength is large enough, and several sub-resonance state will appear near the primary resonance regime. The resonance properties of MCR are essentially different from the side-coupled single-ring resonator in this case. It's worth noting that the transmission near a resonant state changes not only with the detuning of transmission phase, but also drastically with the change of coupling coefficient. A new idea for resonant cavity sensing may be provided based on this characteristic. That is to say, for an intensity-variation sensing scheme base on the MCR, there will be an enhancement term in the sensitivity compared to the side-coupled single-ring resonator when the

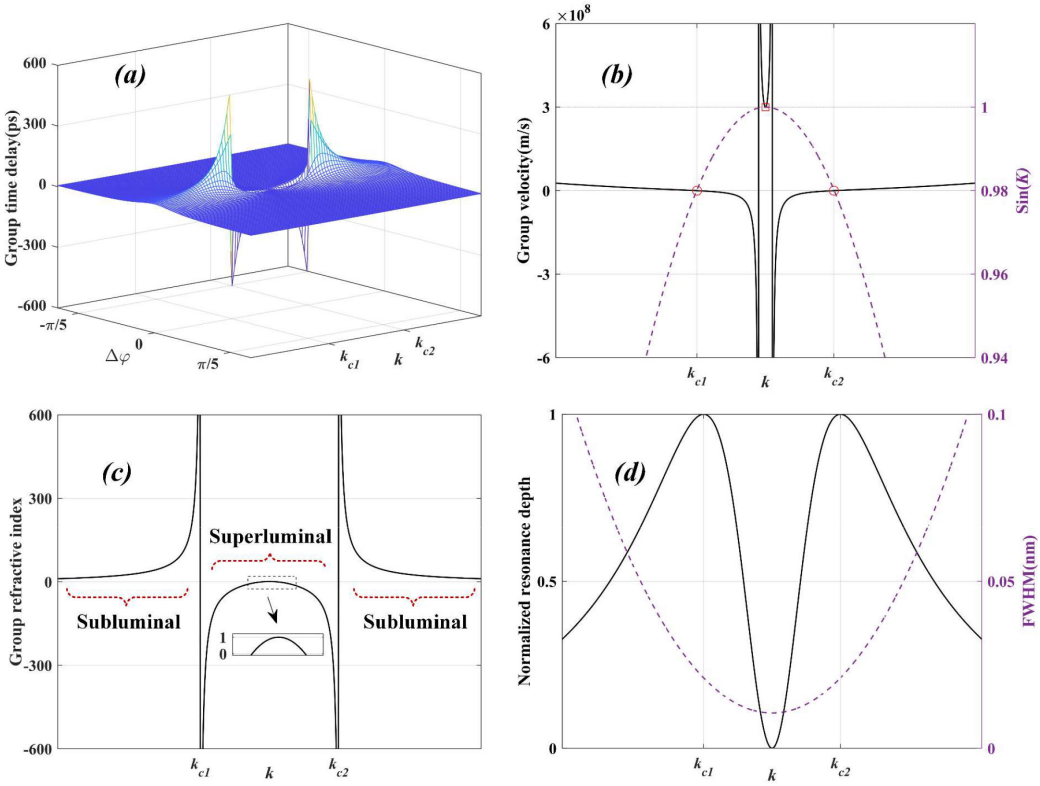

Fig. 3. The evolutions of (a): group delay, (b): group velocity and coupling strength, (c): group refractive index, (d): resonance depth and FWHM of the MCR at primary resonant near a pair of critical-coupling coefficients when $L = 1mm$and $\alpha = 0.02/mm$ are assumed.

detected parameter causes the change of both transmission phase and coupling condition simultaneously.

For an MCR with two turns, the resonance phase is shifted only by 2π periodically in the same resonance condition, and the resonance characteristics such as FSR and FWHM have not been changed, although the coupling coefficient has increased. When the number of turns is more than two and the coupling coefficient is comparatively small, the resonance spectrum still has a regular profile, as indicated by the red arrow in each sub-image of Fig. 2. It means that the similar resonance spectrum can always be obtained for an MCR with any number of turns, as long as the coupling coefficient is set properly. Thus, the transmission characteristics of MCR with several turns are similar to those of the side-coupled single-ring resonator when the coupling coefficient between the adjacent microfibers is relatively small. However, more turns, more coupling times, thus more coupling loss will be induced. When the coupling coefficient is relatively large, just like reveal in Fig. 1 of reference [20], the resonance spectrum becomes no longer pure, and more transmission dips appear in one FSR. The reason is that complex multi-beam interference will be introduced because of the inter-turn coupling propagation of light simultaneously among more than two microfiber turns. It is worth noting that the optimal primary resonance dips always appear in pairs with the change of the coupling coefficient, which means that there are two critical-coupling coefficients near a resonant condition. Critical-coupling means that the internal resonator loss is exactly equal to the coupling loss in an optical resonator, and the transmittance goes to 0 at resonant phases due to perfect destructive interference [33]. The cyclicity of coupling strength, which can be characterized as $\mathrm{Sin}(k \cdot L_{eff})$, indicates this phenomenon is reasonable, and there will be two *k* satisfying the critical-coupling condition in a full coupling period as shown in Fig. 3(b), which can be expressed as:

$$\mathrm{Sin}(K) = \mathrm{Sin}(k_c \cdot L_{eff}) = e^{-\alpha \cdot L_{eff}} \tag{8}$$

where K represents the coupling parameter of the MCR, k_c is the critical-coupling coefficient and $e^{-\alpha \cdot L_{eff}}$ is the amplitude attenuation. Assuming that the amplitude transmission coefficient T in equation (3) is equal to 0 in the resonant phase, and combined with equation (1) and (2), the critical-coupling coefficient of MCR under fundamental resonance condition of K can be derived reversely. For an MCR with 2 turns, the critical-coupling coefficient k_{2c} can be given by:

$$k_{2c_1} = \frac{2\arctan\left(e^{L\alpha} - \sqrt{e^{2L\alpha} - 1}\right) + 2\pi z_1}{L} \tag{9a}$$

or

$$k_{2c_2} = \frac{2\arctan\left(e^{L\alpha} + \sqrt{e^{2L\alpha} - 1}\right) + 2\pi z_1}{L} \tag{9b}$$

For an MCR with 3 turns, the critical-coupling coefficient k_{3c} can be given by:

$$k_{3c_1} = \frac{\sqrt{2}\mathrm{arccot}\left(\sqrt{2}e^{L\alpha} + \sqrt{e^{2L\alpha} - 1}\right) + \sqrt{2}\pi z_2}{L} \tag{10a}$$

or

$$k_{3c_2} = \frac{\sqrt{2}\mathrm{arccot}\left(\sqrt{2}e^{L\alpha} - \sqrt{e^{2L\alpha}-1}\right) + \sqrt{2}\pi z_2}{L} \quad (10b)$$

where z_1 and z_2 are integers respectively. However, for an MCR with more than 3 turns, it is difficult to obtain the analytical solution of k_c due to the complexity of the transfer matrix, and only an approximate numerical solution can be obtained in this case.

III. Superluminal and Subluminal Propagation in Different Coupling Conditions

For the sake of analysis, only the primary resonant regime under the fundamental resonant condition is considered in this section. The dependence of group delay on the detuning of transmission phase $\Delta\varphi$ and the coupling coefficient deviating from the critical value k_c is shown in Fig. 3(a), where k_{c1} is the smaller of a pair of critical-coupling coefficients under primary resonant condition, and k_{c2} is the larger one. Reasonably, the magnitude of the group delay is much larger near resonance (i.e., $\Delta\varphi = 0$). Moreover, the positive and negative group delays, which correspond to the normal and anomalous dispersion, are observed successively near critical-coupling. For a more intuitive explanation of the dependence of group dispersion on coupling condition, the corresponding evolutions of group velocity and group refractive index near the critical-coupling coefficients pair k_{c1} and k_{c2} are simulated as shown in Fig. 3(b) and (c), and the coupling strength $\mathrm{Sin}(K)$ as a reference is also exhibited by the dotted line in Fig. 3(b), where the critical and fully coupling conditions are indicated by circles and square, respectively. As thus, the region between k_{c1} and k_{c2} represents over-coupling, and the other region represents under-coupling. It can be seen that the corresponding group delay, group velocity and group refractive index are all positive in the under-coupling region. The extreme value of group delay is obtained near critical-coupling, and abrupt change between positive and negative values. In fact, this extreme value should be infinite theoretically (only the extreme value of about 510 is shown due to the limitation of simulation accuracy), because the light is completely trapped in the MCR just like other resonators. Expectedly, the group velocity will be zero in this case as indicated by circles in Fig. 3(b). Correspondingly, the evolution of group refractive index near the critical-coupling is exhibited in Fig. 3(c). The evolution of group refractive index with coupling strength is consistent almost with that of the group delay. The positive group velocity in under-coupling condition, which is initially less than the speed of light in vacuum, decreases gradually to 0 with the coupling strength increasing to critical value. This situation corresponds to normal dispersion and subluminal propagation. As a contrast, the dependence of group velocity on coupling strength becomes more sensitive when $\mathrm{Sin}(K)$ is larger than the critical value. With the increase of the coupling strength exceeding the critical value, the group velocity firstly drops rapidly to a negative extreme value, and then abrupt changes to a positive extreme value. Whereas with the further increase of coupling strength, the infinite positive group velocity drops sharply to the speed of light in vacuum at full-coupling point ($\mathrm{Sin}(K) = 1$) as indicated by square in Fig. 3(b). In this paper, positive group velocity less than the speed of light in vacuum and negative group velocity are both referred to as superluminal propagation, and anomalous dispersion regime is obtained in this case. This feature may suggest potential applications in the spontaneous emission noise of lasers [13]. It should be noted that the abrupt change point of the positive and negative group delay is at the critical-coupling, while the abrupt change point of the positive and negative group velocity is not so, but at a certain point of over-coupling. It corresponds to the point where group refractive index is equal to 0 as revealed by the zoom-in superluminal propagation region in Fig. 3(c).

The evolutions of resonance depth and full width at half maximum (FWHM) near the critical-coupling are also calculated as shown in Fig. 3(d). The resonance depth, which corresponding to the index of signal-to-noise ratio in sensing applications, reaches its maximum at critical-coupling and minimum at full-coupling. The FWHM, which corresponding to the detection limit assessment in sensing applications, decreases with the coupling strength increasing, and reaches its minimum at full coupling. However, it is meaningless because the resonance depth is also infinitesimal, and the MCR is equivalent to an all-pass filter in this case. It is more reasonable to operate the MCR in slight over-coupling condition corresponding with the negative superluminal propagation. On the whole, superluminal propagation means a narrower FWHM, but there should be a tradeoff between it and a higher resonance depth.

It is necessary to explore the effect of loss on superluminal and subluminal propagation. For simplicity, only the group refractive index is exhibited to characterize the superluminal and subluminal propagation regime, and the dependences of group refractive index on loss coefficient is simulated in an MCR with only two turns, because the results in other cases are similar. The effect of loss on the group refractive index in different coupling conditions are shown in Fig. 4, where k_c is obtained by equation 9 and 10 with respect to different loss coefficient. Obviously, it is different that the effect of loss on superluminal and subluminal propagation regime in different coupling conditions. In under-coupling condition ($k = 0.95k_c$, as shown by the red dotted line in Fig. 4(b)), the positive group refractive index decreases with the loss increasing. Therefore, subluminal propagation regime can always be obtained when the MCR is operated in under-coupling condition.

By comparison, the evolution of group refractive index groups with increasing loss is not monotone in both critical-coupling ($k = k_c$, as shown by the black solid line in Fig. 4(a)) and over-coupling condition ($k = 1.05k_c$, as shown by the blue solid line in Fig. 4(b)), rather than there is a loss threshold near which the group refractive index changes dramatically. At these respective thresholds, the negative group index abrupt change to positive in critical-coupling condition while the positive group index abrupt change to negative in over-coupling condition. Nevertheless, the loss threshold in the case of critical-coupling is as small as $10^{-8}\mathrm{mm}^{-1}$ orders of magnitude, which is impossible in the current micro-fiber manufacturing technology. This threshold

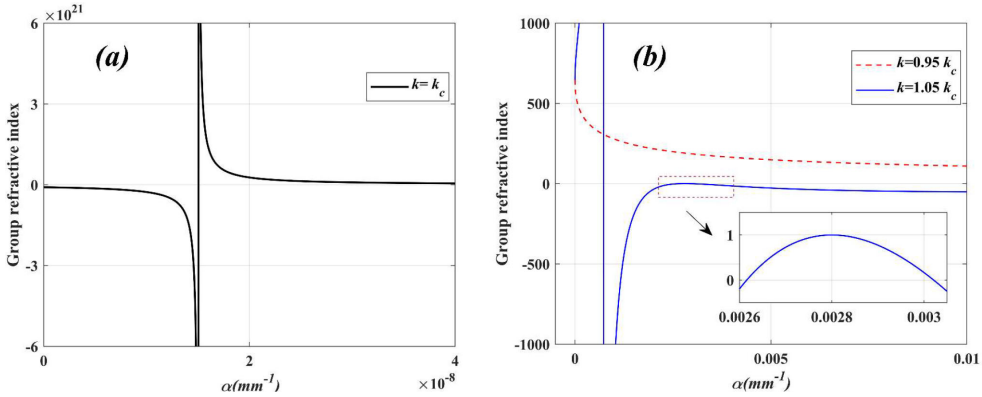

Fig. 4. The dependence of group refractive index of the MCR at primary resonant on the loss at (a): critical-coupling condition ($k = k_c$), (b): under-coupling condition ($k = 0.95k_c$) and over-coupling condition ($k = 1.05k_c$).

is increased by 10^5 orders of magnitude in the case of over-coupling, which is about 10^{-3}mm^{-1}, and it is much more practical in the manufacturing process. Compared with group refractive indices of 10^2 magnitude in under-coupling condition, it can be up to 10^{21} magnitude in critical-coupling condition. Therefore, it is more efficient to operate MCR in critical-coupling condition to obtain a sufficiently strong subluminal propagation, and a sufficiently small loss is required. Some enlightenment may be brought for further optimized design of micro-resonators to meet specific requirements, such as in dispersion compensation, optical storage and optical switching [20], [34]. Particularly, positive group refractive index less than 1 is obtained in a certain loss range (0.0026∼0.003mm^{-1}) as shown in the partial zoom of the blue solid lines. It means that a precise coordination of the loss coefficient and the coupling coefficient is required for obtaining positive superluminal propagation.

IV. Potential Sensitivity Enhancement of Biochemical and Inertial Sensing

Considerable research has been done experimentally and theoretically on the sensing mechanism based on a ring resonator operated in superluminal or subluminal propagation regime [35]. It is generally acknowledged that subluminal propagation means stronger light–matter interaction because of the larger group delay, and the more time for light to propagate in the resonator. Therefore, the resonator operated in subluminal propagation regime is more suitable for biochemical sensing [22], [36]. In contrast, light–matter interaction is weak when the ring resonator is operated in superluminal propagation regime, and it is more beneficial to be applied to inertial sensing [37]. As one of the most sensitive optical sensing methods, phase shift readout scheme is widely used in resonator sensing. For biochemical sensing, it relies on evanescent wave sensing to interrogate the presence of analytes around the resonator waveguide. The existence of analytes modulates the refractive index of resonator waveguide cladding, and the effective index of the guided mode also is modulated accordingly. Then, the phase shift of incident beam passing through the resonator will be read out as a mapping of the refractive index change of the analytes. As a whole, the transmission phase shift of the resonator is modulated by the analytes, which is finally converted into the difference of the output optical intensity. So, the sensitivity can be expressed as the differential of the output optical intensity to the change in the waveguide parameter affected by the measurand. For simplicity, the change of refractive index of resonator waveguide cladding in biochemical sensing scheme is considered as a reference:

$$S_R = \frac{\partial I(\varphi)}{\partial n_0} = \frac{\partial I(\varphi)}{\partial \varphi} \cdot \frac{\partial \varphi}{\partial n_0} = \frac{\partial I(\varphi)}{\partial n_{eff}} \cdot \frac{\partial n_{eff}}{\partial n_0} \tag{11}$$

where $\varphi = k_0 \centerdot n_{eff} \centerdot l$ is the transmission phase, k_0 is the wavenumber, l is the perimeter of ring resonator, n_0 is the refractive index of analyte, n_{eff} is effective index of the guided mode in resonator. $I(\varphi)$ represents that the measured optical intensity is a function of transmission phaseφ.

Interestingly, for an MCR, not only the effective index of the guided mode is modulated, but also the coupling condition in MCR is adjusted by the change of the refractive index of analyte. The reason is that compared with the edge-coupled single-ring resonator, the MCR has much more coupling regions relies on the evanescent inter-turn coupling between the adjacent microfibers in a helical coil configuration, that is to say, the coupling occurs in the whole resonator. Fig. 2 has demonstrated the transmission near a resonant state changes not only with the detuning of transmission phase, but also drastically with the change of coupling coefficient. Furthermore, the evolution of the transmittance with the coupling coefficient near the resonance is different when the number of turns is different. Especially for the MCR with more than 2 turns, the multiple resonant dips make it more complicated. A potential sensitivity enhancement based on this characteristic can be provided. Therefore, the sensitivity based on an MCR should be expressed as:

$$S_{R\_MCR} = \frac{\partial I(\varphi, k)}{\partial n_0} = \frac{\partial I(\varphi, k)}{\partial \varphi} \cdot \frac{\partial \varphi}{\partial n_0} + \frac{\partial I(\varphi, k)}{\partial k} \cdot \frac{\partial k}{\partial n_0} \tag{12}$$

where $I(\varphi, k)$ represents that the measured optical intensity is a function of transmission phaseφ and the coupling coefficient k. It means that the biochemical sensing based on an MCR has a sensitivity enhancement term $\frac{\partial I(\varphi,k)}{\partial k} \cdot \frac{\partial k}{\partial n_0}$. What's more, the

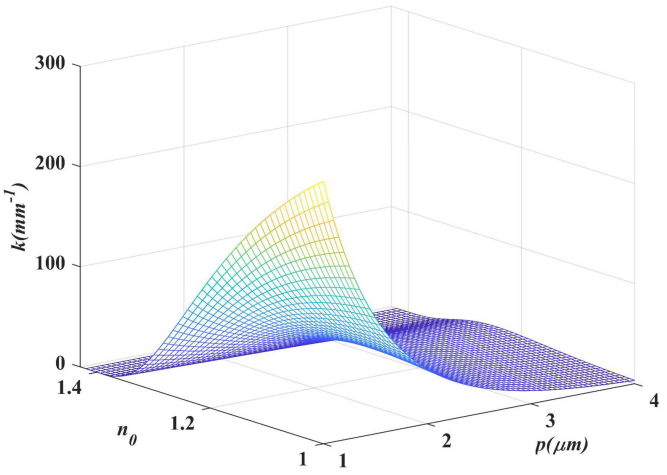

Fig. 5. The dependences of coupling coefficient k on the cladding refractive index n_0 and the pitch p between adjacent microfibers.

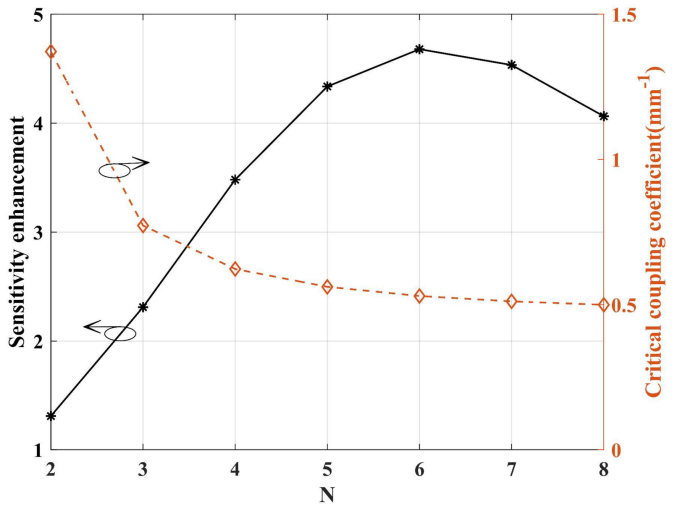

Fig. 6. Sensitivity enhancement and critical-coupling coefficients of the MCR with different turns.

coupling coefficient between two adjacent microfibers is related to the cladding refractive index, which can be written as:

$$k=\frac{\sqrt{\Delta}}{r}\frac{u^2}{V^3K_1^3(w)}\sqrt{\frac{\pi r}{wp}}\exp\left(-\frac{w}{r}p\right) \tag{13}$$

where $w=r\sqrt{\beta^2-k_0^2n_0^2}$ and $u=r\sqrt{k_0^2n_1^2-\beta^2}$ represent the normalized transverse wavenumbers, respectively. $V=\sqrt{u^2+w^2}$ is the normalized frequency, andK_1 is the modified Bessel function of the first kind. Δ can be obtained by $n_1^2-n_0^2=2n_1^2\Delta$, r and p are the microfiber radius and the pitch between adjacent microfibers respectively as marked in Fig. 1.

Fig. 5 depicts the dependences of coupling coefficient on the cladding refractive index n_0 and the pitch between adjacent microfibers with 1μm diameter. When the pitch is 1, that is, two adjacent microfibers are close to each other, the coupling coefficient can be as large as about 300mm^{-1}, and it decreases rapidly with the increase of pitch. Moreover, the smaller the pitch, the sharper the coupling coefficient changes with cladding refractive index n_0. The pitch should be small enough in the practical MCR sensing configuration. Notice that the change of coupling coefficient with the cladding refractive index tends to be blunt when n_0 is near 1.4, that is, near the refractive index of microfiber. The reason is that the inter-turn coupling is weakened when the refractive index of cladding is close to that of micro fiber, and the two adjacent microfibers are almost equivalent to merging into one microfiber. Therefore, it is more effective to operate in the regime where the refractive index of cladding is far from that of micro-fiber for such a sensor configuration.

In view of the complexity of the transmission near different critical-coupling coefficients for MCR with more than 2 turns, only the case of minimum critical-coupling, as indicated by the arrow in Fig. 2, is considered for simplicity, although the transmission dip is much steeper in the case of larger critical-coupling. Fig. 6 reveals that sensitivity enhancement and critical-coupling coefficients of the MCR with different turns. It should be pointed that here the sensitivity enhancement is expressed by the ratio of the sensitivity considering both the transmission phase and the coupling in MCR with different turns to the sensitivity considering only the transmission phase in MCR with 2 turns. Because it is difficult to find the analytical solution for the critical-coupling of MCR with more than 3, the critical-coupling coefficients of MCR with more than 3 turns are obtained by approximate numerical calculation. The cladding (i.e., the analytic) refractive index varies around 1.3 is assumed, and the effective index of the guided mode n_{eff} with different cladding refractive index are obtained by semi-vector finite difference mode method [38]. The sensitivity enhancement can be as large as 4.7 in an MCR with 6 turns, however, it is not increasing further for an MCR with more turns. The reason is that the critical-coupling coefficient has not been further reduced significantly, while the coupling loss increases ceaselessly with the number of turns, which restricts the sensitivity enhancement. Actually, for an MCR with more turns operating at a larger critical-coupling point, the evolution of transmission with the coupling becomes much sharper, and the sensitivity enhancement can be more multiples because of a larger sensitivity enhancement term $\frac{\partial I(\varphi,k)}{\partial k}$.

For inertial sensing, compared with the change of cladding refractive index in biochemical sensing, the optical path of the beams propagating in the resonator will be modified by the measurand, such as acceleration or angular velocity. Hence the transmission phase shift of the resonator is modulated similarly. Furtherly, the coupling length, which is closely related to the coupling condition, will also be adjusted by the change of optical path. Therefore, the transmission of MCR will also be modulated collectively by the detuning of transmission phase and coupling, and it is predictable the result of sensitivity enhancement is similar to that of the biochemical sensing. For example, the optical path difference between two beams propagating in clockwise and counterclockwise directions will be caused by angular velocity, which will cause resonant phase splitting (equivalent to resonance frequency splitting) in two different directions, i.e., Sagnac effect [39], [40]. The angular velocity can be interrogated by detecting the output optical intensity difference of the two

different directions, and the sensitivity can be expressed as:

$$S_{\Omega\_MCR} = \frac{\partial I(\delta\omega, K)}{\partial \Omega} = \frac{\partial I(\delta\omega, K)}{\partial \delta\omega} \cdot \frac{\partial \delta\omega}{\partial \Omega} + \frac{\partial I(\delta\omega, K)}{\partial K} \cdot \frac{\partial K}{\partial \Omega} \quad (14)$$

where Ω and $\delta\omega$ are respectively angular velocity and the Sagnac frequency splitting caused by rotation, and:

$$\delta\omega = \frac{\omega_0 \cdot R}{c \cdot n_g}\Omega \quad (15)$$

where $\omega_0$is resonant frequency of the resonator at stationary state [41]. Hence the angular velocity sensing based on an MCR has a sensitivity enhancement term $\frac{\partial I(\delta\omega,K)}{\partial K} \cdot \frac{\partial K}{\partial \Omega}$. Also notice that the Sagnac frequency splitting is inversely proportional to the group refractive index n_g, thus it is more appropriate to operate the MCR under the condition of positive superluminal regime, as indicated in Fig. 3(c) and Fig. 4(b).

V. Conclusion

In this paper, the resonance characteristics near critical-coupling condition of the MCR with different turns is presented firstly. For the primary resonant regime, the FSR is independent of the number of turns, which indicates that the beam does not propagate spirally along the microfiber in the MCR, and the effective length of the MCR is constant. The resonance dips always appear in pairs corresponding to multiple critical-coupling because of the periodicity of coupling strength, and critical-coupling coefficient expressions of the MCR with 2 and 3 turns are derived. However, complicated resonance is observed in an MCR with larger coupling coefficient and turns.

By adjusting the coupling condition, superluminal or subluminal propagation can be obtained respectively. As a whole, the dispersion response of the primary resonant regime is similar to that of the single-ring resonator. The under-coupling condition corresponds to normal dispersion and subluminal propagation, and the positive group velocity below the velocity of light in vacuum is observed. The over-coupling condition corresponds to anomalous dispersion and superluminal propagation, and the positive group velocity above the velocity of light and the negative group velocity are observed. The maximum resonant depth is obtained at critical-coupling, and the FWHM decreases with the increase of the coupling strength, hence there should be a tradeoff between a higher resonance depth and a narrower FWHM. The effect of loss on superluminal and subluminal propagation under different coupling condition is also explored. The response of the superluminal and subluminal propagation regime on the loss in different coupling conditions is different. There is such a loss threshold in the critical-coupling and over-coupling conditions, near which the group refractive index abrupt changes between positive and negative extremum, and the threshold is increased by 10^5 orders of magnitude under over-coupling condition compared with critical-coupling. A precise coordination of the loss coefficient and the coupling coefficient is required for obtaining positive superluminal propagation. The subluminal propagation regime can always be obtained when the MCR is operated in under-coupling condition, and very little loss is required to obtain a sufficiently strong subluminal propagation.

Due to the much more coupling regions relies on the evanescent inter-turn coupling between the adjacent microfibers in a helical coil configuration, and the transmission near a resonant state evolve not only with the detuning of transmission phase, but also drastically with the adjustment of coupling condition which will be modulated by the cladding refractive index and coupling length, thus a potential sensitivity enhancement for resonant cavity sensing may be provided based on this characteristic. The sensitivity enhancement can be as large as 4.7 in an MCR with 6 turns for biochemical sensing, and the sensitivity enhancement can be larger for an MCR with more turns operating at a larger critical-coupling point. It is predictable that the result of sensitivity enhancement for inertial sensing is similar, and operating the MCR in positive superluminal propagation regime is more appropriate because of the weak light–matter interaction and the enhancement from positive group refractive index below 1. A series of experiments will be carried out to verify these inferences in the following work, and it is hoped that this study can provide theoretical assistance for the practical application of MCR.

References

[1] L. M. Tong *et al.*, "Subwavelength-diameter silica wires for low-loss optical wave guiding," *Nature,* vol. 426, no. 6968, pp. 816–819, Dec. 2003.

[2] M. Sumetsky, Y. Dulashko, J. M. Fini, A. Hale, and D. J. DiGiovanni, "The microfiber loop resonator: Theory, experiment, and application," *J. Lightw. Technol.,* vol. 24, no. 1, pp. 242–250, Jan. 2006.

[3] L. Shi, Y. Xu, W. Tan, and X. Chen, "Simulation of optical microfiber loop resonators for ambient refractive index sensing," *Sensors,* vol. 7, no. 5, pp. 689–696, May, 2007.

[4] X. Jiang *et al.*, "Demonstration of optical microfiber knot resonators," *Appl. Phys. Lett.,* vol. 88, no. 22, 2006.

[5] M. Sumetsky, "Optical fiber microcoil resonator," *Opt. Exp.,* vol. 12, no. 10, pp. 2303–2316, 2004.

[6] K. J. Vahala, "Optical microcavities," *Nature,* vol. 424, no. 6950, pp. 839–846, 2003.

[7] M. Sumetsky, "Basic elements for microfiber photonics: Micro/nanofibers and microfiber coil resonators," *J. Lightw. Technol.,* vol. 26, no. 1, pp. 21–27, Jan. 2008.

[8] T.-H. Shen and L. A. Wang, "A two-layer microcoil resonator with very high quality factor," *IEEE Photon. Technol. Lett.,* vol. 26, no. 6, pp. 535–537, Mar. 2014.

[9] Y.-C. Hsieh, T.-S. Peng, and L. A. Wang, "Millimeter-sized microfiber coil resonators with enhanced quality factors by increasing coil numbers," *IEEE Photon. Technol. Lett.,* vol. 24, no. 7, pp. 569–571, Apr. 2012.

[10] F. Xu, P. Horak, and G. Brambilla, "Optimized design of microcoil resonators," *J. Lightw. Technol.,* vol. 25, no. 6, pp. 1561–1567, Jun. 2007.

[11] F. Xu, P. Horak, and G. Brambilla, "Conical and biconical ultra-high-Q optical-fiber nanowire microcoil resonator," *Appl. Opt.,* vol. 46, no. 4, pp. 570–573, Feb. 2007.

[12] M. Arjmand, V. Ahmadi, and M. Karimi, "Wavelength-Selective optical amplifier based on microfiber coil resonators," *J. Lightw. Technol.,* vol. 30, no. 16, pp. 2596–2602, Aug. 2012.

[13] T. Laupretre, S. Schwartz, R. Ghosh, I. Carusotto, F. Goldfarb, and F. Bretenaker, "Anomalous ring-down effects and breakdown of the decay rate concept in optical cavities with negative group delay," *New J. Phys.,* vol. 14, pp. 13, Apr. 2012.

[14] M. Stenner, D. J. Gauthier, and M. A. Neifeld, "Fast causal information transmission in a medium with a slow group velocity," *Phys. Rev. Lett.,* vol. 94, no. 5, 2005, Art. no. 053902.

[15] D. Dahan and G. Eisenstein, "Tunable all optical delay via slow and fast light propagation in a raman assisted fiber optical parametric amplifier: A route to all optical buffering," *Opt. Exp.*, vol. 13, pp. 6234–6249, 2005.

[16] Y. A. Vlasov, M. O'Boyle, H. F. Hamann, and S. J. Mcnab, "Active control of slow light on a chip with photonic crystal waveguides," *Nature,* vol. 438, no. 7064, pp. 65–69, 2005.
[17] S. Wang, L. Ren, L. Yu, and Y. Tomita, "Zero-broadening SBS slow light propagation in an optical fiber using two broadband pump beams," *Opt. Exp.,* vol. 16, no. 11, pp. 8067–8076, 2008.
[18] C. N. Alexeyev, A. V. Milodan, M. C. Alexeyeva, and M. A. Yavorsky, "Inversion of the topological charge of optical vortices in a coil fiber resonator," *Opt. Lett.,* vol. 41, no. 7, pp. 1526–1529, Apr. 2016.
[19] F. Xu, Q. Wang, J.-F. Zhou, W. Hu, and Y.-Q. Lu, "Dispersion study of optical nanowire microcoil resonators," *IEEE J. Sel. Top. Quantum Electron.,* vol. 17, no. 4, pp. 1102–1106, Jul./Aug. 2011.
[20] N. G. R. Broderick, "Optical snakes and ladders: Dispersion and nonlinearity in microcoil resonators," *Opt. Exp.,* vol. 16, no. 20, pp. 16247–16254, Sep. 2008.
[21] A. Kowsari, V. Ahmadi, G. Darvish, and M. K. Moravvej-Farshi, "Dynamic analysis of optical microfiber coil resonators," *Appl. Opt.,* vol. 55, no. 24, pp. 6680–6687, Aug. 2016.
[22] C.-J. Ma, L.-Y. Ren, Y.-P. Xu, Y.-L. Wang, and H. Zhou, "Theoretical and experimental study of structural slow light in a microfiber coil resonator," *Appl. Opt.,* vol. 54, no. 18, 2015.
[23] F. Xu, P. Horak, and G. Brambilla, "Optical microfiber coil resonator refractometric sensor," *Opt. Exp.,* vol. 15, no. 12, 2007, Art. no. 7888.
[24] X. Y. Lu and L. A. Wang, "A refractive index sensor based on a packaged microfiber coil resonator," in *Proc. Int. Conf. Opt. MEMS Nanophot. (OMN)*, 2017, pp. 1–2.
[25] F. Xu and G. Brambilla, "Demonstration of a refractometric sensor based on optical microfiber coil resonator," *Appl. Phys. Lett.,* vol. 92, no. 10, Mar. 2008.
[26] J. M. López-Higuera *et al.*, "Single-polarization microfiber and resonator for sensing applications," in *Proc. 23rd Int. Conf. Opt. Fibre Sensors*, vol. 9157, 2014, pp.1–4.
[27] S. Zhu, L. Shi, N. Liu, X. Xu, and X. Zhang, "Magnetic field sensing using magnetic-fluid-filled optofluidic ring resonator," *Microfluid. Nanofluid.,* vol. 21, no. 10, Oct. 2017.
[28] J. Scheuer, "Fiber microcoil optical gyroscope," *Opt. Lett.,* vol. 34, no. 11, pp. 1630–1632, Jun. 2009.
[29] G. Brambilla *et al.*, "Optical fiber nanowires and microwires: Fabrication and applications," *Adv. Opt. Photon.,* vol. 1, no. 1, pp. 107–161, 2009.
[30] G. Lenz, B. Eggleton, C. K. Madsen, and R. Slusher, "Optical delay lines based on optical filters," *IEEE J. Quantum Electron.,* vol. 37, no. 4, pp. 525–532, Apr. 2001.
[31] M. Sumetsky, "Uniform coil optical resonator and waveguide: Transmission spectrum, eigenmodes, and dispersion relation," *Opt. Exp.,* vol. 13, no. 11, pp. 4331–4340, May 2005.
[32] C. Ma, L. Ren, and Y. Xu, "Slow-light element for tunable time delay based on optical microcoil resonator," *Appl. Opt.,* vol. 51, no. 26, pp. 6295–6300, 2012.
[33] A. Yariv, "Universal relations for coupling of optical power between microresonators and dielectric waveguides," *Electron. Lett.,* vol. 36, no. 4, pp. 321–322, Feb. 2000.
[34] V. S. Ilchenko, A. A. Savchenkov, A. B. Matsko, and L. Maleki, "Dispersion compensation in whispering-gallery modes," *J. Opt. Soc. Amer. a-Opt. Image Sci. Vis.,* vol. 20, no. 1, pp. 157–162, Jan. 2003.
[35] N. Y. Liu, L. Shi, S. Zhu, X. B. Xu, S. X. Yuan, and X. L. Zhang, "Whispering gallery modes in a single silica microparticle attached to an optical microfiber and their application for highly sensitive displacement sensing," *Opt. Exp.,* vol. 26, no. 1, pp. 195–203, Jan. 2018.
[36] J. Scheuer, G. T. Paloczi, J. Poon, and A. Yariv, "Coupled resonator optical waveguides: Toward the slowing and storage of light," *Opt. Photon. News,* vol. 16, no. 2, 2005.
[37] M. S. Shahriar, G. S. Pati, R. Tripathi, V. Gopal, M. Messall, and K. Salit, "Ultrahigh enhancement in absolute and relative rotation sensing using fast and slow light," *Phys. Rev. A,* vol. 75, no. 5, 2007.
[38] A. B. Fallahkhair, K. S. Li, and T. E. Murphy, "Vector finite difference modesolver for anisotropic dielectric waveguides," *J. Lightw. Technol.,* vol. 26, no. 11, pp. 1423–1431, Jun. 2008.
[39] E. J. Post, "Sagnac effect," *Rev. Mod. Phys.,* vol. 39, no. 2, pp. 475–493, 1967.
[40] W. Yu, Z. Xu, R. Yun-Jiang, G. Yuan, H. Chang-Lun, and Y. Guo-Guang, "MOEMS accelerometer based on microfiber knot resonator," *IEEE Photon. Technol. Lett.,* vol. 21, no. 20, pp. 1547–1549, Oct. 2009.
[41] R. Novitski, J. Scheuer, B. Z. Steinberg, and IEEE, "Modeling sagnac effect in micro resonators using FDTD method," in *Proc. IEEE Photon. Conf.*, 2012, pp. 139–140.